Bis(phosphane)copper(I) and silver(I) dithiocarbamates: crystallography and anti-microbial assay

Nazzatush Shimar Jamaludin,[I] Siti Nadiah Abdul Halim[I] Chai-Hoon Khoo,[II] Bao-Jing Chen,[II] Tian-Hong See,[II] Jiun-Horng Sim,[II] Yoke-Kqueen Cheah,[II,*] Hoi-Ling Seng[III] and Edward R. T. Tiekink[IV,*]

[I] University of Malaya, Department of Chemistry, 50603 Kuala Lumpur, Malaysia

[II] University Putra Malaysia, Department of Biomedical Science, Faculty of Medicine and Health Sciences, 43400 Serdang, Selangor Darul Ehsan, Malaysia

[III] Sunway University, Faculty of Science and Technology, 47500 Bandar Sunway, Selangor Darul Ehsan, Malaysia

[IV] Sunway University, Centre for Crystalline Materials, Faculty of Science and Technology, 47500 Bandar Sunway, Selangor Darul Ehsan, Malaysia

Received; accepted

Keywords: Copper(I) / silver(I) / dithiocarbamate / crystal structure analysis / X-ray diffraction

Abstract. The crystal and molecular structures of $(Ph_3P)_2M[S_2CN(Me)CH_2CH_2OH]$, M = Cu, isolated as a 1:1 dichloromethane solvate (**1**.CH_2Cl_2), and M = Ag (**4**) show the central metal atom to be coordinated by a symmetrically (**1**.CH_2Cl_2) and asymmetrically chelating (**4**) dithiocarbamate ligand. The distorted tetrahedral geometries are completed by two PPh_3 ligands. The presence of hydroxyl-O–H···S(dithiocarbamate) hydrogen bonds leads to centrosymmetric dimeric aggregates in each crystal structure. In the molecular packing of **1**.CH_2Cl_2, channels comprising **1** are formed via aryl-C–H···O interactions with the solvent molecules associated with the walls of the channels via methylene-C–H···S, π(aryl) interactions. For **4**, the dimeric aggregates are connected via a network of aryl-C–H···π(aryl) interactions. Preliminary screening for anti-microbial activity was conducted. The compounds were only potent against Gram-positive bacteria. Some further selectivity in activity was noted. Most notably, all compounds were active against methicillin resistant *Staphylococcus aureus*.

* Correspondence authors: E-mail: ykcheah@medic.upm.edu.my (Y.-K.C.); edwardt@sunway.edu.my (E.R.T.T.)

Introduction

In response to increasing bacterial resistance, perhaps over-prescription of anti-biotics, certainly wide-use and incorrect disposal, and emerging new infections, the once effective anti-microbial drugs are becoming less efficacious posing great challenges in human health [1-4]. In a very recent *Nature* Editorial on the subject, copper and silver were specifically mentioned as providing hope in developing new and effective anti-microbial agents [5]. With the above in mind, it is not surprising that both copper and silver, as nanoparticles and incorporated in molecules, have attracted considerable attention of those developing metal-based therapeutics as summarised in a number of recent reviews [6-10].

The utility of a full range of transition metal and main group element dithiocarbamates as potential metal-based drugs has been reviewed recently [11]. Prominent amongst these are gold dithiocarbamates, including phosphane gold(I) dithiocarbamates. The exploration of the potential anti-cancer activity of phosphane gold(I) dithiocarbamates dates back over a decade [12] and studies on related compounds continue [13-15]. Recently, phosphanegold(I) dithiocarbamates, functionalised with ethylhydroxy groups, proved to be very effective against breast cancer MCF-7R cell lines and to induce cell death (apoptosis or necrosis) via both extrinsic and intrinsic pathways [16]. The same dithiocarbamate ligands when complexed to bismuth(III) [17] and zinc(II) [18] also provide cytotoxic compounds. Over and above displaying interesting cytotoxicity profiles, phosphanegold(I) dithiocarbamates also display potential as anti-microbial agents; see [19] for a recent review on the utility of gold compounds in this context. Interestingly, for these $R_3PAu[S_2CN(iPr)CH_2CH_2OH]$ compounds, activity was found to be dependent on the nature of the phosphane-bound R substituent. Thus, when R = Ph and Cy, specific activity against Gram-positive bacteria was observed but, when R = Et, broad range activity against both Gram-positive and Gram-negative activity was noted. Further, the latter compound proved to be very effective, at least in the chosen in vitro models, against methicillin resistant *Staphylococcus aureus* (MRSA) [20]. A further differential was observed in that R = Ph and Cy compounds were uniformly bactericidal against susceptible bacterial strains, whereas the R = Et derivative was variously bactericidal and bacteriostatic.

Given the foregoing, namely the pharmaceutical interest in copper(I) and silver(I) compounds, and the potential of metal dithiocarbamate compounds in tackling bacteria, it was thought of interest to explore the utility of phosphane copper and silver compounds of dithiocarbamates functionalised with ethylhydroxy substituents in this context. Herein, the synthesis, characterisation, including two crystal structure determinations, and results of preliminary anti-bacterial screening for a series of six compounds of the

general formula, $(Ph_3P)_2M[S_2CN(R)CH_2CH_2OH]$, Fig. 1, are reported.

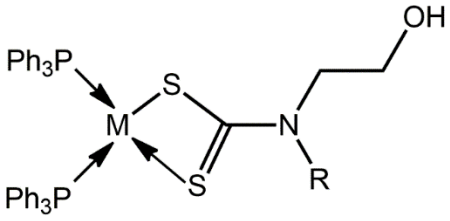

M/R	Me	iPr	CH_2CH_2OH
Cu	**1**	**2**	**3**
Ag	**4**	**5**	**6**

Fig. 1. Chemical structures of the copper(I) and silver(I) compounds investigated herein.

Experimental

Instrumentation

Elemental analyses were performed on a Perkin Elmer PE 2400 CHN Elemental Analyser. ^1H and $^{13}C\{^1H\}$ NMR spectra were recorded in d^6-DMSO solution on a Bruker Avance 400 MHz NMR spectrometer with chemical shifts relative to tetramethylsilane as the internal reference. IR spectra were measured using an Attenuated Technique Reflectance (ATR) on a Perkin Elmer Spectrum 2000 spectrophotometer in the region 400 to 4000 cm^{-1}.

Synthesis and characterisation

$[(Ph_3P)_2Cu\{S_2CN(Me)CH_2CH_2OH\}]$ (1): A modified procedure from the literature [21] was employed. Thus, CuCl (Aldrich, 1 mmol; 0.099 g) was stirred with triphenylphosphane (Aldrich, 2 mmol) in acetone (20 ml) at 323 K until a white precipitate was obtained. Then, an aqueous solution of $K[S_2CN(Me)CH_2CH_2OH]$ [16] (1 mmol) was added to the reaction mixture followed by stirring for 1 h. The product underwent solvent extraction with chloroform:water (1:3), filtered and dried at room temperature. The precipitate was then washed in diethyl ether under vigorous stirring and filtered. Recrystallisation was performed in acetone via quick evaporation at ambient temperature to yield a white solid. Crystals were then obtained from the same solvent by slow evaporation. M. pt: 428 K. Yield: 0.58 g; 78%. Elemental analyses (%): Found C, 64.99; H, 5.04; N; 1.78. $C_{40}H_{38}CuNOP_2S_2$ re-

quires: C, 64.98; H, 5.32; N, 1.89. IR (cm^{-1}): ν(O–H) 3353 (m); ν(C–N) 1432 (m); $\nu(C–S)_{asym}$ 1092 (m, sh); $\nu(C–S)_{asym}$ 992 (m). $^{13}C\{^1H\}$ NMR: 207.0 (S_2C); 128.3-134.0 (aryl-C); 61.1 (OCH_2); 56.7 (NCH_2); 31.1 (CH_3) ppm. $^{31}P\{^1H\}$: -1.26 ppm.

[(Ph_3P)$_2$Cu{$S_2CN(iPr)CH_2CH_2OH$}] (2):
Synthesis and crystallisation was as for **1** but using $Na[S_2CN(iPr)CH_2CH_2OH]$ [16] as the dithiocarbamate ligand. M. pt: 448 K. Yield: 0.54 g; 70%. Elemental analyses (%): Found C, 65.56; H, 5.51; N, 1.69. $C_{42}H_{42}CuNOP_2S_2$ requires: C, 65.73; H, 5.65; N, 1.83. IR (cm^{-1}): ν(O–H) 3467 (m); ν(C–N) 1432 (m); $\nu(C–S)_{asym}$ 1092 (m, sh); $\nu(C–S)_{asym}$ 993 (m). $^{13}C\{^1H\}$ NMR: 209.8 (S_2C); 128.9-134.5 (aryl-C); 63.4 (OCH_2); 52.1 (NCH_2); 48.8 (CH); 20.3 (CH_3) ppm. $^{31}P\{^1H\}$: -1.78 ppm.

[(Ph_3P)$_2$Cu{$S_2CN(CH_2CH_2OH)_2$}] (3):
Synthesis and crystallisation was as for **1** but using $K[S_2CN(CH_2CH_2OH)_2]$ [16]. M. pt: 437 K. Yield: 0.58 g; 75%. Elemental analyses (%): Found C, 63.39; H, 5.28; N, 1.61. $C_{41}H_{40}CuNO_2P_2S_2$ requires: C, 64.00; H, 5.37; N, 1.82. IR (cm^{-1}): ν(O–H) 3353 (m); ν(C–N) 1432 (m); $\nu(C–S)_{asym}$ 1094 (m, sh); $\nu(C–S)_{asym}$ 993 (m). $^{13}C\{^1H\}$ NMR: 208.7 (S_2C); 128.9-134.5 (aryl-C); 58.7 (OCH_2); 56.0 (NCH_2) ppm. $^{31}P\{^1H\}$: -1.03 ppm.

[(Ph_3P)$_2$Ag[$S_2CN(Me)CH_2CH_2OH$}] (4):
A modified literature method [22] was employed whereby $AgNO_3$ (Fluka, 1 mmol; 0.14 g) was stirred with triphenylphosphane (2 mmol) in acetone (20 ml) in a 1:2 ratio at room temperature until a suspension was obtained. Then, $K[S_2CN(Me)CH_2CH_2OH]$ [16] (1 mmol) in water (20 ml) was added to the reaction mixture which was stirred for 1 h. Chloroform was added and stirring was continued for another 1 h, after which the yellow chloroform solution was separated from the aqueous layer. After drying over anhydrous sodium sulphate, the solution was filtered and quickly evaporated to yield a white solid. The solid was washed with diethyl ether and was isolated through filtration. Recrystallisation was performed in acetone via slow evaporation, yielding colourless blocks. M. pt: 444 K. Yield: 0.60 g; 76%. Elemental analyses (%): Found C, 61.30; H, 4.86; N, 1.87. $C_{40}H_{38}CuNOP_2S_2$ requires: C, 61.30; H, 5.02; N, 1.79. IR (cm^{-1}): ν(O–H) 3360 (br); ν(C–N) 1432 (m, sh); $\nu(C–S)_{asym}$ 1094 (m, sh); $\nu(C–S)_{asym}$ 983 (m). $^{13}C\{^1H\}$ NMR: 208.0 (S_2C); 127.3-135.0 (aryl-C); 60.1 (OCH_2); 54.7 (NCH_2); 29.1 (CH_3) ppm. $^{31}P\{^1H\}$: 4.43 ppm.

[(Ph_3P)$_2$Ag{$S_2CN(iPr)CH_2CH_2OH$}] (5):
Synthesis and crystallisation was as for **4** but using $Na[S_2CN(iPr)CH_2CH_2OH]$ [16] as the dithiocarbamate ligand. M. pt: 425 K. Yield: 0.57 g; 70%. Elemental analyses (%): Found C, 62.13; H, 4.95; N, 1.73. $C_{42}H_{42}CuNOP_2S_2$ requires: C, 62.14; H, 5.34; N, 1.73. IR

(cm^{-1}): ν(O–H) 3384 (br); ν(C–N) 1434 (m); $\nu(C–S)_{asym}$ 1092 (m, sh); $\nu(C–S)_{asym}$ 971 (w). $^{13}C\{^1H\}$ NMR: 211.2 (S_2C); 128.3-134.2 (aryl-C); 63.1 (OCH_2); 54.8 (NCH_2); 49.5 (CH); 20.3 (CH_3) ppm. $^{31}P\{^1H\}$: 5.30 ppm.

$[(Ph_3P)_2Ag[S_2CN(CH_2CH_2OH)_2]$ (6):
Synthesis and crystallisation was as for **4** but using $K[S_2CN(CH_2CH_2OH)_2]$ [16]. The crystals were obtained from a chloroform:acetone (1:1 v/v) mixture by slow evaporation. M. pt: 435 K. Yield: 0.63 g; 77%. Elemental analyses (%): Found C, 60.34; H, 5.00; N, 1.44. $C_{40}H_{38}CuNOP_2S_2$ requires: C, 60.52; H, 5.08; N, 1.72. IR (cm^{-1}): ν(O–H) 3322 (br); ν(C–N) 1434 (m, sh); $\nu(C–S)_{asym}$ 1094 (m, sh); $\nu(C–S)_{asym}$ 983 (w). $^{13}C\{^1H\}$ NMR: 211.0 (S_2C); 128.7-133.9 (aryl-C); 60.0 (OCH_2); 58.8 (NCH_2) ppm. $^{31}P\{^1H\}$: 5.80 ppm.

Crystal structure determination

Crystals suitable for crystallography of **1** were grown by the slow evaporation of its dichloromethane solution and were characterised crystallographically as the 1:1 dichloromethane solvate. Crystals of **4** were grown by slow evaporation of its acetone solution. Intensity data for **1** and **4** were measured at 100 K on a Bruker SMART APEX-II CCD diffractometer with graphite-monochromatised Mo Kα radiation (λ = 0.71073 Å). Data processing was with APEX2 and SAINT [23] and the absorption correction was conducted with SADABS [24]. Details of unit cell data, X-ray data collection and structure refinement are given in Table 1. The structures were solved by direct methods [25]. Full-matrix least-squares refinement on F^2 with anisotropic displacement parameters for all non-hydrogen atoms was performed with SHELXL-2014/7 [26]. The C-bound H atoms were placed on stereochemical grounds and refined in the riding model approximation with U_{iso} = 1.2-1.5U_{eq}(carrier atom). For **1**, the O-bound H atom was included in its calculated position with U_{iso} = 1.5U_{eq}(O). Owing to poor agreement, a number of reflections, i.e. (0 1 0; affected by the beam-stop), (2 -10 11), (-8 -9 4), (-1 10 11), (-1 9 10), (-4 11 11), (10 -15 4), (-6 6 4) and (9 -15 6), were omitted from the final cycles of refinement. The maximum and minimum residual electron density peaks of 1.06 and 0.48 $Å^{-3}$, respectively, were located 0.75 and 0.61 Å from the H3A and O1 atoms, respectively. For **4**, two positions were resolved for the O1-CH_2CH_2O chain of the dithiocarbamate ligand. These were refined with distance restraints O–C, N–C and C–C of 1.42, 1.47 and 1.52 Å, respectively. The major component of the disordered chain has a site occupancy factor = 0.683(7). The hydroxyl-H atom was included in the model with O–H = 0.84±0.01 Å and with U_{iso} = 1.5U_{eq}(O). Only one position was included for this atom (at full weight) as this was located in a chemically sensible position based on hydrogen bonding consid-

erations. This gives rise to a PLATON [27] alert owing to an impossibly close contact with an H atom of the minor component of the disorder. A weighting scheme of the form $w = 1/[\sigma^2(F_o^2) + (aP)^2]$ where $P = (F_o^2 + 2F_c^2)/3$ was introduced in each case. The final difference maps were featureless. The programs WinGX [28], ORTEP-3 for Windows [28] {at the 70% probability level} and DIAMOND [29] were also used in the study.

Table 1. Crystallographic data and refinement details for **1**.CH_2Cl_2 and **4**.[a]

Compound	(**1**.CH_2Cl_2)	(**4**)
Formula	$C_{40}H_{38}CuNOP_2S_2$, CH_2Cl_2	$C_{40}H_{38}AgNOP_2S_2$
Formula weight	823.24	782.64
Colour, habit	Colourless, prism	Colourless, prism
Dimensions/mm	0.07 x 0.07 x 0.12	0.18 x 0.20 x 0.30
Crystal system	triclinic	monoclinic
Space group	$P\bar{1}$	$P2_1/c$
a/Å	12.3145(7)	13.6595(5)
b/Å	12.8280(6)	10.1048(4)
c/Å	13.7989(13)	25.5522(10)
α/°	97.894(5)	90
β/°	93.688(5)	95.127(2)
γ/°	115.535(3)	90
V/Å^3	1929.6(2)	3512.8(2)
Z/*Z*′	2/1	4/1
D_c/g cm^{-3}	1.417	1.480
F(000)	852	1608
μ(Mo*K*α)/mm^{-1}	0.930	0.818
Measured data	18472	32615
Data completeness	1.00	1.00
R_{int}	0.050	0.091
θ range/°	1.9–27.5	1.5–27.5
Unique data	8815	8057
Observed data [$I \geq 2.0\sigma(I)$]	6370	5779
R, obs. data; all data	0.048; 0.072	0.044; 0.072
a in weighting scheme	0.049	0.029
GoF	1.03	1.01
R_w, obs. data; all data	0.108; 0.122	0.081; 0.092

a Supplementary Material: Crystallographic data for the structures reported in this paper have been deposited with the Cambridge Crystallographic Data Centre as supplementary publications no. CCDC-1437530 and 1437530. Copies of available material can be obtained free of charge, on application to CCDC, 12 Union Road, Cambridge CB2 1EZ, UK, (fax: +44-(0)1223-336033 or e-

mail: deposit@ccdc.cam.ac.uk). The list of Fo/Fc-data is available from the corresponding author (ERTT) up to one year after the publication has appeared.

Evaluation of in vitro anti-microbial activity

Microorganisms

The bacteria tested in this study were *Aeromonashydrophilla* (*A. hydrophilla*) ATCC35654, *Acinetobacterbaumannii* (*A. baumannii*) ATCC 19606, *Bacillus cereus* (*B. cereus*) ATCC 10876, *Bacillus subtilis* (*B. subtilis*) ATCC 6633, *Citrobacterfreundii* (*C. reundii*) ATCC 8090, *Enterobacter cloacae* (*E. cloacae*) ATCC 35030, *Enterobacteraerogenes* (*E. aerogenes*) ATCC 13048, *Enterococcus faecalis* (*E. faecalis*) ATCC 29212, *Enterococcus faecium* (*E. faecium*) ATCC 19434, *Escherichia coli* (*E. coli*) ATCC 25922, *Klebsiella pneumoniae* (*K. pneumoniae*) ATCC 700603, *Listeria monocytogenes* (*L. monocytogenes*) ATCC 19117, *Proteus mirabilis* (*P. mirabilis)* ATCC25933, *Proteus vulgaris* (*P. vulgaris*) ATCC 13315, *Pseudomonas aeruginosa* (*P. aeruginosa*) ATCC27853, *Salmonella paratyphi* A (*S. paratyphiA*) ATCC 9150, *Salmonella typhimurium* (*S. typhimurium*) ATCC 14028, *Shigellaflexneri* (*S. flexneri*) ATCC 12022, *Shigellasonnei* (*S. sonnei*) ATCC 9290, *Staphylococcus aureus* (*S. aureus*) ATCC 25923, methicillin resistant *Staphylococcus aureus* (MRSA) ATCC 43300, *Staphylococcus saprophyticus* (*S. saprophyticus*) ATCC 15305, *Stenotrophomonasmaltophilia* (*S. maltophilia*) ATCC 13637 and *Vibrio parahaemolyticus* (*V. parahaemolyticus*) ATCC17802. All bacterial cultures were purchased from American Type Culture Collection (ATCC).

Screening of anti-bacterial activity

Anti-bacterial screening was performed using the Kirby-Bauer disc diffusion method in accordance with the National Committee for Clinical Laboratory Standards (NCCLS) guideline. The inoculum suspension of each bacterial strain was adjusted to 0.5 McFarland standard turbidity (corresponds to approximately 10^8 CFU/ml) by adding Mueller-Hinton broth (Difco, USA). Then, this suspension was swabbed on the surface of Mueller-Hinton agar (MHA; Difco, USA) plates. The tested compounds were dissolved in DMSO to a test concentration of 10 mg/ml. Sterile 6 mm filter paper discs were aseptically placed on Mueller-Hinton agar surfaces and 5 µl of each of the dissolved compounds was immediately added to the discs. Each plate contained one standard anti-biotic paper disc which served as the positive control, one disc served as negative control (5 µl broth) and one disc served as solvent control (5 µl DMSO). The plates were incubated at 37 °C for 24 h. The anti-bacterial activity was evaluated by measuring the diameter of inhibition zone against the test bacterial strains. Each trial was performed in duplicate.

Results and discussion

Synthesis and characterisation

Compounds **1**–**6** were obtained in good yields from the facile metathetical reaction between the respective copper(I) or silver(I) salt with an alkali metal salt of the dithiocarbamate anion. Characteristic absorption bands due to ν(C–N) and ν(C–S) of the dithiocarbamate ligands were observed in their IR spectra. The $^{13}C\{^{1}H\}$ NMR showed the expected resonances due to the phosphane and dithiocarbamate ligands. Finally, the $^{31}P\{^{1}H\}$ NMR showed singlets a few ppm downfield for the copper(I) compounds, and upfield for the silver(I) compounds. The appearance of singlets is consistent with rapid exchange of the phosphane ligands in solution [30]. Full structure determination for two species, namely **1**.CH_2Cl_2 and **4** were afforded by X-ray crystallography.

Crystal and molecular structure of 1.CH_2Cl_2

The molecular structures in **1**.CH_2Cl_2 are shown in Fig. 2 and selected geometric parameters are collected in Table 2. The copper(I) atom is chelated by the dithiocarbamate ligand and the tetra-coordinate geometry is completed by two triphenylphosphane (Ph_3P) ligands. The dithiocarbamate is chelating in the symmetric mode with Cu–S1, S2 being experimentally equivalent at 2.4171(9) and 2.4190(8), respectively; the symmetric Cu–S bond lengths are also reflected in the experimental equivalence of the associated C1–S1, S2 bond lengths of 1.719(3) and 1.727(3), respectively. There are significant deviations from the ideal tetrahedral angle of 109.5º, most notably in the acute chelate angle of 75.03(3)º and the wide angle subtended by the bulky Ph_3P ligands of 124.09(3)º. While the S1–Cu–P1, P2 angles of 112.88(3) and 109.50(3) are close to each other and to the ideal tetrahedral values, the S2–Cu–P1, P2 angles, i.e. 125.64(3) and 99.13(3)º, differ from each other by over 25º. Based on the value calculated for τ_4, a four-coordinate geometry index [30], i.e. 0.78 cf. 1 for an ideal tetrahedron, the coordination geometry is best described as distorted tetrahedral.

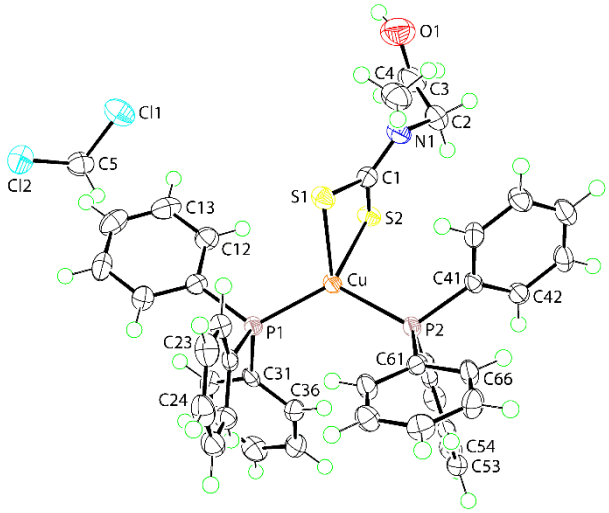

Fig. 2. Molecular structures in **1**.CH_2Cl_2. Displacement ellipsoids are drawn at the 70% probability level.

The molecular structure of **1** in **1**.CH_2Cl_2 complements a number of literature precedents [32-36] for which geometric data are collated in Table 2. Noteworthy, is the structure of $[(Ph_3P)_2Cu\{S_2CN(CH_2CH_2OH)_2\}]$, as its triphenylphosphane lattice adduct, which corresponds to **3** in the present report. All structures are relatively homogeneous in that all adopt the distorted tetrahedral geometry, as in **1**.CH_2Cl_2, with a symmetric mode of coordination of the dithiocarbamate ligand, and a wide angle subtended by the phosphane ligands. However, non-systematic variations in other angles subtended at the copper(I) centre are evident, Table 2.

The most prominent supramolecular aggregation in the crystal structure of **1**.CH_2Cl_2 is based on hydroxyl-O–H···S(dithiocarbamate) hydrogen bonding which leads to a centrosymmetric dimer, Fig. 3a; geometric data characterising supramolecular interactions for both **1**.CH_2Cl_2 and **4** are listed in Table 3. Globally, dimeric aggregates stack in columns along the *a*-axis and define channels in which reside the dichloromethane molecules, Fig. 3b. Connections between molecules of **1** are of the type aryl-C–H···O(hydroxyl), and the solvent is attached to the inside of the channels via methylene-C–H…S and methylene-C–H···π(aryl) interactions.

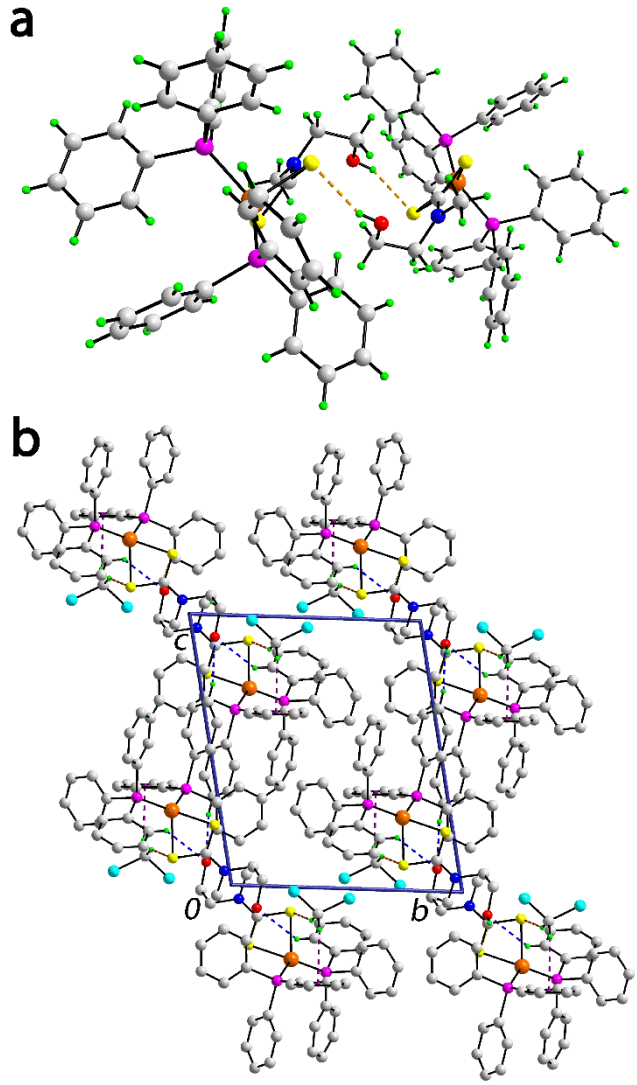

Fig. 3. Molecular packing in **1**.CH_2Cl_2: (a) view of the supramolecular dimeric aggregate sustained by O–H…S hydrogen bonding (orange dashed lines), and (b) view in projection of the unit cell contents down the *a*-axis. The C–H…S, C–H…O and C–H…π interactions are shown as brown, blue and purple dashed lines, respectively. For the packing diagram, only hydrogen atoms involved in the discussed intermolecular interactions are included.

Table 2. Selected geometric parameters (Å, º) for **1**.CH_2Cl_2, **4** and literature precedents.

Structure	Cu–S1, S2	Cu–P1, P2	S1–Cu–S2	P1–Cu–P2	S1–Cu–P1, P2	S2–Cu–P1, P2	τ_4	Ref.
1.CH_2Cl_2	2.4171(9), 2.4190(8)	2.2418(8), 2.2778(9)	75.03(3)	124.09(3)	112.88(3), 109.50(3)	125.64(3), 99.13(3)	0.78	This work
$[(Ph_3P)_2Cu\{S_2CN(CH_2CH_2OH)_2\}]$[a]	2.3948(11), 2.4288(11)	2.2594(13), 2.2849(14)	74.76(4)	124.52(5)	112.35(4), 109.85(4)	122.04(4), 102.50(4)	0.81	32
$[(Ph_3P)_2Cu\{S_2CN(n\text{-}Pr)_2\}]$[b]	2.4036(17), 2.4063(14)	2.2516.(15), 2.2764(15)	74.56(5)	124.09(6)	119.67(5), 106.03(6)	110.73(5), 111.11(5)	0.82	33
$[(Ph_3P)_2Cu\{S_2CN(CH_2CH_2)_2S\}]$[b]	2.3808(10), 2.4063(9)	2.2556(9), 2.2651(9)	75.14(3)	125.85(3)	113.89(3), 113.39(4)	112.20(3), 104.05(3)	0.85	34
$[(Ph_3P)_2Cu\{S_2CN(CH_2CH_2)_2NPh\}]$[c]	2.3887(12), 2.4055(10)	2.2700(14), 2.2347(11)	75.03(4)	119.36(4)	113.94(4), 115.94(4)	102.46(4), 121.79(4)	0.84	34
	2.3956(12), 2.4167(10)	2.2299(11), 2.2661(14)	74.77(4)	122.49(4)	113.87(4), 108.32(4)	126.31(4), 100.88(4)	0.79	
$[(Ph_3P)_2Cu\{S_2CN(Me)CH_2Ph\}]$[b]	2.3974(14), 2.4021(12)	2.2382(17), 2.2604(19)	75.30(4)	124.86(6)	110.15(5), 118.32(5)	109.72(5), 106.63(5)	0.83	35
$[(Ph_3P)_2Cu\{S_2CN(CH_2Ph)CH_2py\text{-}4\}]$[d]	2.406(2), 2.4166(16)	2.275(2), 2.263(2)	74.60(6)	123.95(7)	111.45(7), 117.66(7)	112.73(6), 105.02(7)	0.84	36
4	2.5945(9), 2.7074(10)	2.4577(9), 2.4824(9)	68.18(3)	124.36(3)	118.89(3), 115.57(3)	109.29(3), 100.25(3)	0.83	This work
$[(Ph_3P)_2Ag\{S_2CN(Me)CH_2CH_2OH\}]$[b]	2.6380(9), 2.6592(9)	2.4173(11), 2.4964(11)	68.34(3)	122.53(3)	118.11(3), 108.10(3)	131.93(3), 95.02(3)	0.75	30
$[(Ph_3P)_2Ag\{S_2CN(n\text{-}Bu)CH_2CH_2OH\}]$	2.6091(10), 2.6717(11)	2.4255(13), 2.4658(13)	68.48(3)	123.52(4)	125.31(3), 103.12(4)	114.54(4), 108.66(4)	0.79	30
$[(Ph_3P)_2Ag\{S_2CN(CH_2)_5\}]$	2.5690(10), 2.7082(11)	2.4646(9), 2.4756(8)	68.15(3)	124.43(3)	117.86(3), 114.53(3)	108.11(3), 107.23(3)	0.84	37

a Crystallised as a 1:1 Ph_3P lattice adduct. *b* Crystallised as a 1:1 dichloromethane solvate. *c* Two independent molecules in the asymmetric unit. *d* Crystallised as a dihydrate.

Table 3. Summary of intermolecular interactions (A–H…B; Å, º) operating in the crystal structures of **1**.CH_2Cl_2 and **4**.[a]

A	H	B	A–H	H…B	A…B	A–H…B	Symmetry operation
(**1**)							
O1	H1o	S2	0.84	2.41	3.207(4)	159	1-*x*, 2-*y*, -*z*
C12	H12	O1	0.95	2.58	3.270(5)	129	1-*x*, 2-*y*, -*z*
C54	H54	O1	0.95	2.47	3.409(4)	169	*x*, *y*, 1+*z*
C5	H5a	S1	0.99	2.85	3.752(4)	152	1+*x*, *y*, *z*
C5	H5b	Cg(C61-C66)	0.99	2.73	3.553(4)	140	1+*x*, *y*, *z*
(**4**)							
O1	H1o	S2	0.84(3)	2.55(3)	3.387(4)	174(3)	2-*x*, 2-*y*, 2-*z*
C25	H25	Cg(C61-C66)	0.95	2.77	3.635(4)	151	*x*, 1½-*y*, ½+*z*
C34	H34	Cg(C41-C46)	0.95	2.91	3.554(4)	126	1-*x*, -½+*y*, 1½-*z*
C45	H45	Cg(C51-C56)	0.95	2.86	3.425(4)	119	2-*x*, ½+*y*, 1½-*z*

a Cg is the ring centroid of the specified atoms.

Crystal and molecular structure of 4

The molecular structure of **4** is shown in Fig. 4 and selected geometric parameters are given in Table 2. To a first approximation, the molecular structure is the same as for **1** in **1**.CH_2Cl_2 with the notable difference being that the dithiocarbamate ligand in **4** coordinates in an asymmetric mode whereby the difference between the Ag–S1, S2 bond lengths is greater than 0.10 Å. This change results in a contraction of the chelate angle subtended by the dithiocarbamate-sulphur atoms. Based on the value computed for τ_4, i.e. 0.83, the coordination geometry is less distorted from the ideal tetrahedral geometry compared with **1** in **1**.CH_2Cl_2.

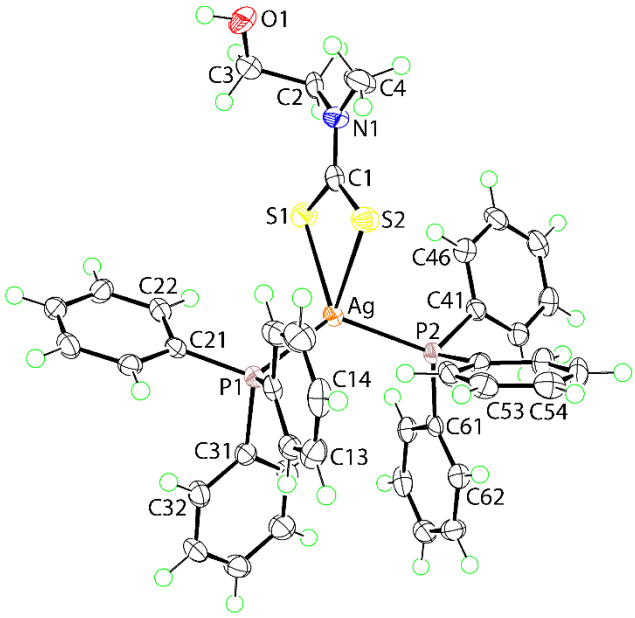

Fig. 4. Molecular structure of **4**. Displacement ellipsoids are drawn at the 70% probability level. Only the major component of the disordered O1-hydroxyethyl group is shown.

There are three literature precedents for $(Ph_3P)_2Ag(S_2CNR_2)$ [30, 37], including a very recently reported structure for **4** but, as its dichloromethane solvate [30]; see Table 2 for salient geometric data. A comparison of the key geometric parameters for **4** and **4**.CH_2Cl_2 [30] clearly confirms the flexibility in this class of molecule as, for example, the Ag–S bond lengths in **4**.CH_2Cl_2 differ by only 0.02 Å cf. 0.10 in **4**. This is opposite to the trends in the Ag–P bond lengths for which the difference was 0.02 Å in **4** but, this expands to 0.08 Å in **4**.CH_2Cl_2. There are also considerable differences in the angles subtended at the silver(I) centre with the range being 10° greater in **4**.CH_2Cl_2. The value of τ_4 in **4**.CH_2Cl_2 is 0.75 revealing this structure to exhibit the greatest deviation from tetrahedral behaviour of all structures listed in Table 2.

Further, a comment of the isostructural relationships is appropriate. It is noted that six out of the ten structures included in Table 2 have occluded dichloromethane in their crystal structures. Indeed, for the silver(I) series, the pair of solvated compounds ($P\bar{1}$) are isostructural as is the pair of unsolvated compounds ($P2_1/c$). The unit characteristics of three of the dichloromethane solvates in the copper(I) series are also isostructural with their silver(I) counterparts, the exceptional structure being that of $\{(Ph_3P)_2Cu[S_2CN(CH_2CH_2)_2S]\}$ [33] which has monoclinic ($P2_1/c$) symmetry.

As for **1**.CH_2Cl_2, the formation of a centrosymmetric supramolecular dimer stabilised by hydroxyl-O–H···S(dithiocarbamate) hydrogen bonding is the most conspicuous feature of the molecular packing of **4**, Fig. 5a and Table 3. The dimers stack in columns along the *b*-axis and are consolidated into the three-dimensional architecture by aryl-C–H···π(aryl) interactions, Fig. 5b.

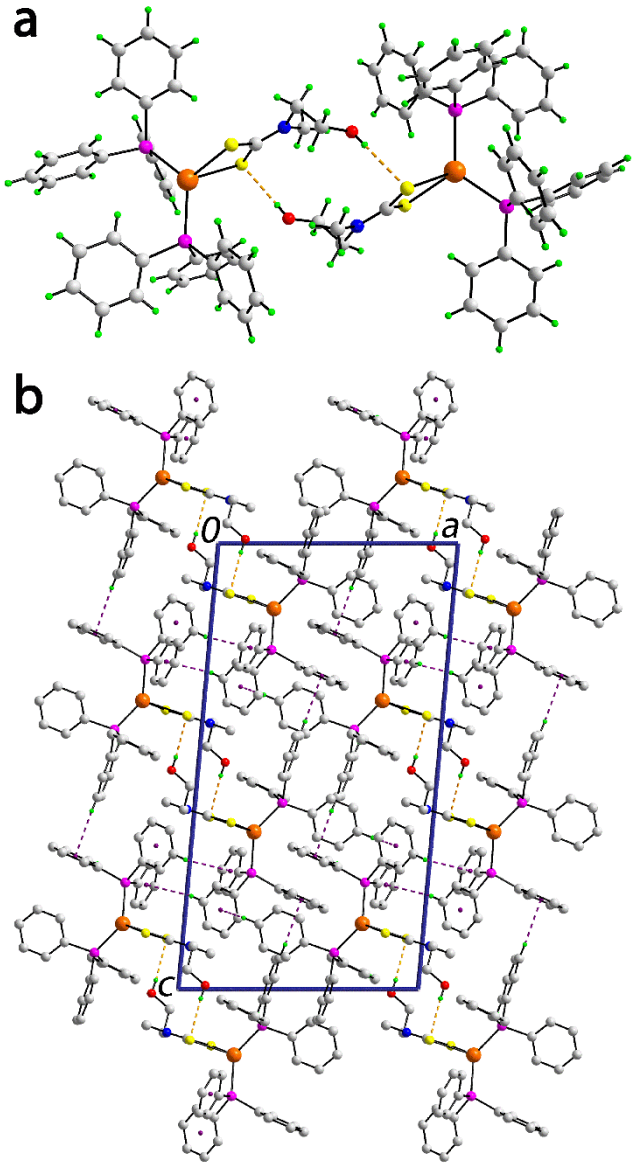

Fig. 5. Molecular packing in **4**: (a) view of the supramolecular dimeric aggregate sustained by O–H…S hydrogen bonding (orange dashed lines), and (b) view in projection of the unit cell contents down the *b*-axis. The C–H…π interactions are shown as purple dashed lines. For the packing diagram, only hydrogen atoms involved in the discussed intermolecular interactions are included.

It is of interest to note that in each of **1**.CH_2Cl_2 and **4**, hydroxyl-O–H···S(dithiocarbamate) hydrogen bonding is observed rather than the what might be anticipated hydroxyl-O–H···O(hydroxyl) hydrogen bonding, as hydroxyl is both a good donor and acceptor of hydrogen bonds [38, 39]. Mono-alcohols can potentially self-associate via hydroxyl-O–H···O(hydroxyl) hydrogen bonds into zero-dimensional aggregates, such as a dimer or an oligomer, and into one-dimensional supramolecular chains, as illustrated in Fig. 6. Indeed, these modes of supramolecular association have been observed in the crystal structures of related dithiocar-

bamate species. Thus, referring to Fig. 6, the dimer synthon has been found, for example, in $[Zn\{S_2CN(Me)CH_2CH_2OH\}\{3\text{-}NC_5H_4CH_2N(H)C(=O)C(=O)N(H)CH_2C_5H_4N\text{-}3\}]_n$ [40] in one of the supramolecular isomers of $[\{Cd[S_2CN(iPr)CH_2CH_2OH]_2\}_2.2MeCN.2H_2O]_n$ [41] and in 1:2 co-crystal $[\{Cd[S_2CN(iPr)CH_2CH_2OH]_2\}_2$:2[3-(propan-2-yl)-1,3-oxazolidine-2-thione]] [42], and cyclic tetrametric synthons in $[Ni\{S_2CN(iPr)CH_2CH_2OH\}_2]$ [43] and in co-crystal $[Zn\{S_2CN(Me)CH_2CH_2OH\}\{3\text{-}NC_5H_4CH_2N(H)C(=O)C(=O)N(H)CH_2C_5H_4N\text{-}3\}.2S_8]$ [44]. Supramolecular chains have been observed in the structures of $[Zn\{S_2CN(Et)CH_2CH_2OH\}_2]$ [45] and $[Zn\{S_2CN(Me)CH_2CH_2OH\}_2]$ [18]. On the other hand supramolecular chains mediated by hydroxyl-O–H···S(dithiocarbamate) hydrogen bonding have been seen in the aforementioned $R_3PAu[S_2CN(iPr)CH_2CH_2OH]$, R = Et and Cy, structures [16]. Further, charge-assisted hydroxyl-O–H···S^-(dithiocarbamate) hydrogen bonding features prominently in a series of salts of dithiocarbamate anions bearing hydroxylethyl substituents. [46]. The wide range of observed hydrogen bonding patterns in these structures perhaps provides an explanation why disorder in the hydroxyethyl residues is prevalent in these systems.

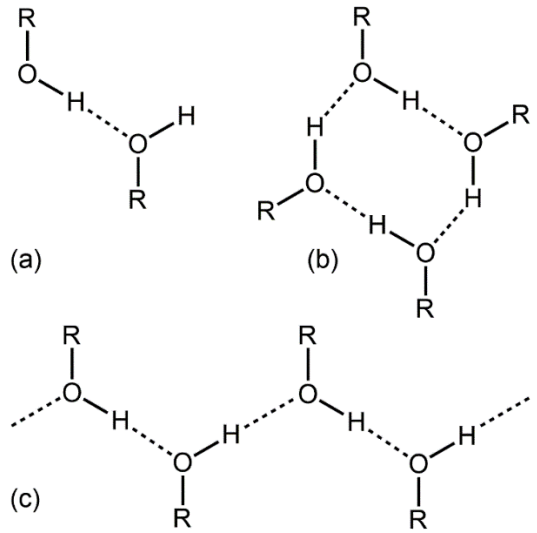

Fig. 6. Common supramolecular synthons found in mono-alcohol crystal structures: (a) zero-dimensional dimer, (b) zero-dimensional oligomer formed by four mono-alcohol molecules, and (c) one-dimensional chain.

Preliminary anti-microbial studies

In the present study, compounds **1**–**6** were screened against a panel of 24 bacteria; the dithiocarbamate ligands themselves are not active. The first key observation was that none of the studied compounds exhibited any activity against Gram-negative bacteria. By contrast, some activity was seen against Gram-positive bacteria with results tabulated in Table 4. A possible explanation for this selectively might relate to the permeability barrier of **1**–**6** since the

structure and properties of the cell membranes of the Gram-positive and Gram-negative bacterial cells are distinct. The outer membrane of Gram-negative bacteria is an asymmetric bilayer, with an inner leaflet comprising phospholipids and the outer leaflet comprising mainly of lipopolysaccharide. The presence of this barrier enables Gram-negative bacteria to overcome harsh environments and to exclude several antibiotics effective against Gram-positive organisms [47].

Amongst the Gram-positive bacteria screened, some selectivity toward bacteria was noted in that **1**–**6** were non-potent against *B. cereus* and *E. faecium*. Only silver compounds were potent against *B. subtilis* (**4** and **6**) and *S. saprophyticus* (**6**), and only compounds with two hydroxyethyl groups (**3** and **6**) were potent against *E. faecalis* and *L. monocytogenes*. By contrast, both copper and silver compounds were active against *S. aureus* (excluding **2**) and *S. aureus (MRSA)*. While some interesting selectivity is noted, none of the compounds was active as the standard antibiotics.

A comment on the potency of related phosphanegold(I) dithiocarbamates, $R_3PAu[S_2CN(iPr)CH_2CH_2OH]$ [20], is apposite. Interestingly, when R = Ph and Cy in this series, selective activity was also seen against Gram-positive bacteria. This observation suggests that the Ph_3P ligand impacts upon the selectivity of metal compound. By contrast, the R = Et compound was active against both Gram-positive and Gram-negative bacteria and generally more potent than the compounds with more bulky phosphane ligands. While all three compounds were active against *S. aureus (MRSA)*, as in the present series of **1**–**6**, the R= Et was particularly potent with a MIC value of 0.98 μg/ml [20].

Table 4 Anti-bacterial activity of **1**–**6** and standard anti-biotics against Gram-positive bacteria as measured by zone of inhibition (mm).[a]

Microorganism	**1**	**2**	**3**	**4**	**5**	**6**	**Anti-biotic** (
B. subtilis ATCC 6633	-	-	-	7	-	7	31[b]
E. faecalis ATCC 29212	-	-	7	-	-	7	12[b]
L. monocytogenes ATCC 19117	-	-	7	-	-	7	27[b]
S. aureus ATCC 25923	8	-	7	8	7	8	17[c]
S. aureus (MRSA) ATCC 43300	8	7	8	8	7	8	15[c]
S. saprophyticus ATCC 15305	-	-	-	-	-	7	30[b]

a The diameter of inhibition zones in millimetres (mm) were measured around the disc after 24 h incubation; –, no zone of inhibition. *b* Tetracycline. *c* Chlorophenicol.

Conclusions

A comparison of newly determined crystal structures of **1**.CH_2Cl_2 and **4** with literature precedents reveal a high degree of concordance in the modes of coordination of the dithiocarbamate ligands in the respective series and common coordination geometries based on a tetrahedral P_2S_2 donor set. In the molecular packing, hydrogen bonding of the type hydroxyl-O–H···S(dithiocarbamate) form in preference to hydroxyl-O–H···S(hydroxyl), and serve to link molecules into centrosymmetric aggregates. While not as potent as standard anti-biotics, compounds **1**–**6** how selectivity toward Gram-positive bacteria and additional selectivity is exhibited depending on i) the central atom, and ii) the nature of the dithiocarbamate-bound substituents. Such results suggest that further investigation of anti-bacterial activity of related systems is warranted.

Acknowledgements. The support from the University of Malaya and the Ministry of Higher Education, Malaysia, High-Impact Research scheme (UM.C/HIR-MOHE/SC/12) is gratefully acknowledged.

References

[1] S. Hemaiswarya, A. K. Kruthiventi, M. Doble, *Phytomedicine* **2008**, *15*, 639.
[2] Editorial, *Nature* **2013**, *495*:141
[3] M. McKenna, *Nature* **2013**, *499*, 394.
[4] B. Mole, *Nature* **2013**, *499*, 398.
[5] Editorial: *Nature* **2015**, *521*, 402.
[6] F. Tisato, C. Marzano, M. Porchia, M. Pellei, C. Santini, *Med. Res. Rev*. **2010**, *30*, 708.
[7] B. Biersack, A. Ahmad, F.H. Sarkar, R. Schobert, *Curr. Med. Chem*. **2012**, *19*, 3949.
[8] S. Eckhardt, P. S. Brunetto, J. Gagnon, M. Priebe, B. Giese, K. M. Fromm, *Chem. Rev*. **2013**, *113*, 4708.
[9] K. Mijnedoncks, N. Leys, J. Mahillon, S. Silver, R. Van Houdt, *Biometals* **2013**, *26*, 609.
[10] C. Santini, M. Pellei, V. Gandin, M. Porchia, F. Tisato, *Chem. Rev*. **2014**, *114*, 815.
[11] G. Hogarth, *Mini-Rev. Med. Chem*. **2012**, *12*, 1202.
[12] D. de Vos, S.Y. Ho and E.R.T. Tiekink, *Bioinorg. Chem. Applns*, **2004**, *2*, 141.
[13] V. Gandin, A. P. Fernandes, M. Pia Rigobello, B. Dani, F. Sorrentino, F. Tisato, M. Björnstedt, A. Bindoli, A. Sturaro, R. Rella, C. Marzano, *Biochem. Pharm*. **2010**, *9*, 90.
[14] F. K. Keter, I. A. Guzei, M. Nell, W. E. van Zyl, J. Darkwa, *Inorg. Chem*. **2014**, *53*, 2058.
[15] M. Altaf, M. Monim-ul-Mehboob, A. A. Isab, V. Dhuna, G. Bhatia, K. Dhuna, S. Altuwaijri, *New. J. Chem.* **2015**, *39*, 377.
[16] N. S. Jamaludin, Z.-J. Goh, Y. K. Cheah, K.-P. Ang, J. H. Sim, C. H. Khoo, Z. A. Fairuz, S. N. B. A. Halim, S. W. Ng, H.-L. Seng, E. R. T. Tiekink, *Eur. J. Med. Chem.* **2013**, *67*, 127.
[17] D. H. A. Ishak, K. K. Ooi, K. P. Ang, A. Md. Akim, Y. K. Cheah, N. Nordin, S. N. B. A. Halim, H.-L. Seng, E. R. T. Tiekink, *J. Inorg. Biochem.* **2014**, *130*, 38.
[18] Y. S. Tan, K. K. Ooi, K. P. Ang, A. Md Akim, Y.-K. Cheah, S. N. A. Halim, H.-L. Seng and E. R. T. Tiekink, *J. Inorg. Biochem.* **2015**, *150*, 48.
[19] B. Đ. Glišić, M. I. Djuran, Dalton Trans. **2014**, *43*, 5950.
[20] J.-H. Sim, N. S. Jamaludin, C.-H. Khoo, Y.-K. Cheah, S. N. B. A. Halim, H.-L. Seng, E. R. T. Tiekink, *Gold Bull*. **2014**, *47*, 225.
[21] M. Afzaal, C. L. Rosenberg, M. A. Malik, A. J. P. White, P. O'Brien, *New J. Chem.* **2011**, *35*, 2773.
[22] R. A. Stein, C. Knobler, *Inorg. Chem.* **1977**, *16*, 242.
[23] Bruker. APEX2 and SAINT. Bruker AXS Inc., Madison, Wisconsin, USA, **2009**.
[24] G. M. Sheldrick, SADABS. University of Göttingen, Germany, **1996**.
[25] G. M. Sheldrick, *Acta Crystallogr. A* **2008**, *64*, 112.
[26] G. M. Sheldrick, *Acta Crystallogr. C* **2015**, *71*, 3.
[27] A. L. Spek, *J. Appl. Crystallogr*. **2003**, *36*, 7.
[28] L. J. Farrugia, *J. Appl. Crystallogr*. **2012**, *45*, 849.
[29] K. Brandenburg, DIAMOND. Crystal Impact GbR, Bonn, Germany, **2006**.
[30] R. Mothes, H. Petzold, A. Jakob, T. Rüffer, H. Lang, *Inorg. Chim. Acta* **2015**, *429*, 227.
[31] L. Yang, D. R. Powell, R. P. House, *Dalton Trans.* **2007**, 955.
[32] F. Jian, F. Bei, L. Lu, X. Yang, X. Wang, I. A. Razak, S. Shanmuga Sundara Raj, H.-K. Fun, *Acta Crystallogr. C* **2000**, *56*, e288.

[33] L. Z. Xu, J. H. Lin, S. S. Zhang, K. Jiao, F. F. Jian, *Pol. J. Chem.* **2001**, *75*, 755.
[34] A. N. Gupta, V. Singh, V. Kumar, A. Rajput, L. Singh, M. G. B. Drew, N. Singh, *Inorg. Chim. Acta* **2013**, *408*, 145.
[35] A. Kumar, H. Mayer-Figge, W. S. Sheldrick, N. Singh, *Eur. J. Inorg. Chem.* **2009**, 2720.
[36] G. Rajput, V. Singh, S. K. Singh, L. B. Prasad, M. G. B. Drew, N. Singh, *Eur. J. Inorg. Chem.* **2012**, 3885.
[37] A. H. Othman, H.-K. Fun, K. Sivakumar, *Acta Crystallogr. C* **1996**, *52*, 843.
[38] M. C. Etter, *Acc. Chem. Res*. **1990**, 23, 120.
[39] C. P. Brock, L. L. Duncan, *Chem. Mat*. **1994**, *6*, 1307.
[40] P. Poplaukhin, E. R. T. Tiekink, *CrystEngComm* **2010**, *12*, 1302.
[41] Y. S. Tan, A. L. Sudlow, K. C. Molloy, Y. Morishima, K. Fujisawa, W. J. Jackson, W. Henderson, S. N. Bt. A. Halim, S. W. Ng, E. R. T. Tiekink, *Cryst. Growth Des*. **2013**, *13*, 3046.
[42] Y. S. Tan, S. N. A. Halim, E. R. T. Tiekink, *Z. Kristallogr. – Cryst. Mat.* **2015**, DOI 10.1515/zkri-2015-1889.
[43] E. R. T. Tiekink, J. L. Wardell, S. M. S. V. Wardell, *J. Chem. Cryst.* **2007**, *37*, 439.
[44] P. Poplaukhin, H. D. Arman, E. R. T. Tiekink, *Z. Kristallogr. – Cryst. Mat.* **2012**, *227*, 363.
[45] R. E. Benson, C. A. Ellis, C. E. Lewis, E. R. T. Tiekink, *CrystEngComm* **2007**, *9*, 930.
[46] R. A. Howie, G. M. de Lima, D. C. Menezes, J. L. Wardell, S. M. S. V. Wardell, D. J. Young and E. R. T. Tiekink, *CrystEngComm* **2008**, *10*, 1626.
[47] E. Freinkman, S. Chng, D. Kahne, *PNAS* **2011**, *108*, 2486.